UDC 533.9

CONFINEMENT PHYSICS OF THE LHD PLASMA AND ITS FUTURE PROSPECT

K.Yamazaki, N.Ashikawa[1], P.deVries, M.Emoto, H.Funaba, M.Goto, K.Ida, H.Idei, K.Ikeda, S.Inagaki, N.Inoue, M.Isobe, S.Kado, O.Kaneko, K.Kawahata, K.Khlopenkov, A.Komori, S.Kubo, R.Kumazawa, S.Masuzaki, T.Minami, J.Miyazawa, T.Morisaki, S.Morita, S.Murakami, S.Muto, T.Mutoh, Y.Nagayama, Y.Nakamura, H.Nakanishi, K.Narihara, Y.Narushima, K.Nishimura, N.Noda, T.Notake 2, T.Kobuchi[1], Y.Liang[1], S.Ohdachi, N.Ohyabu, Y.Oka, M.Osakabe, T.Ozaki, R.O.Pavlichenko, B.J.Peterson, A.Sagara, K.Saito[2], S.Sakakibara, R.Sakamoto, H.Sasao[1], M.Sasao, K.Sato, M.Sato, T.Seki, T.Shimozuma, M.Shoji, H.Suzuki, M.Takechi, Y.Takeiri, N.Tamura[1], K.Tanaka, K.Toi, T.Tokuzawa, Y.Torii[2], K.Tsumori, H.Yamada, I.Yamada, S.Yamaguchi, S.Yamamoto[2], M.Yokoyama, Y.Yoshimura, K.Y.Watanabe, T.Watari, K.Itoh, K.Matsuoka, K.Ohkubo, I.Ohtake, T.Satow, S.Sudo, T.Uda, O.Motojima, Y.Hamada, M.Fujiwara

National Institute for Fusion Science, Oroshi-cho 322-6, Toki, Gifu-ken, 509-5292,Japan
[1] *Graduate University for Advanced Studies, Hayama, 240-0193, Japan*
[2] *Department of Energy Engineering and Science, Nagoya University, Nagoya 464-8603,Japan*

The helical confinement physics is reviewed focused on the present Large Helical Device (LHD) experiments and its future reactor prospect. The LHD experiment shows that the global plasma confinement time is ~1.5-2 times higher than the previous scaling laws. The highest beta value among helical devices (~2.4%) was achieved in LHD. The long pulse (>1 minute) of a keV plasma has been demonstrated. The LHD would confirm the performance potential of a Heliotron configuration towards a steady-state fusion reactor.

1. Introduction

Helical plasma confinement system has a great advantage to keep steady-state plasma without plasma current disruption, and is characterized by favorable current-free magnetic configuration, intrinsic helical divertor concept, and reliable steady-state operation. During the long history of helical confinement research and development (Fig.1), the Large Helical Device (LHD) [1,2] has been constructed as an extension of the Japanese Heliotron concept [3]. After the initial experiment on April,1998, the third cycle experiment has already been

Click to see the picture

Fig.1 Development of Helical Confinement Concept

carried out, and better confinement results than the conventional scalings have been achieved [4].

In this paper, the physics concept of the LHD plasma configuration and its experimental results are given. The future reactor prospect is also described in the final chapter.

2. Physics Design Concept

To demonstrate the above-stated merits of helical system concept, the Large Helical Device (LHD) project has been started with major radius of 3.6-3.9 m, minor radius of 0.6-0.65 m and magnetic field strength of ~ 3 T. The LHD (Fig. 2) is designed on the basis of the following physics criteria [5]: (1) loss-cone-free particle confinement within one-third plasma radius, (2) high beta achievement probability (~5%), and (3) clean helical divertor configuration leading to better confinement properties than the conventional LHD scaling. In order to demonstrate the stead-state plasma operation, the NbTi superconducting helical and poloidal coil system was adopted and successfully operated up to ~3 Tesla. More than one minute plasma duration has been achieved by only NBI or ICRF heating scheme [6].

3. Experimental Achievement Overview

An eight-year construction phase had led to successful engineering commissioning of the device and to start-up of plasma experiments from April 1998. Until now three experimental campaigns have been performed, and the good plasma confinement characteristics has been established so far, with confinement time ~1.5 - 2 times better than several conventional helical scaling laws. The edge plasma behavior and existence of temperature profile pedestal made important effects on the plasma confinement. The dimensionless transport analysis clarified the “strong Gyro-Bohm”-like dependence especially near the plasma edge region. The highest beta value among helical devices has been obtained in LHD. Full steady-state operation has been realized by means of superconducting coil system in addition to physically intrinsic built-in helical divertor.

Fig.2 Large Helical Device (LHD)

The plasma parameters attained so far in LHD are as follows:

(1) higher Te [Te(0) = 4.4 keV
at $\langle n_e \rangle = 5.3 \times 10^{18} m^{-3}$ and P_{abs} = 1.8 MW]

(2) higher confinement [τ_E = 0.3 s,
Te(0) = 1.1 keV at $\langle n_e \rangle = 6.5 \times 10^{19} m^{-3}$
and P_{abs} = 2.0 MW]

(3) highest stored energy [W_{pdia}= 880 kJ],

(4) the highest β value [2.4% at B = 1.3 T], and

(5) longest pulse
[NBI only: τ_{pulse} = 80 s, $T_e(0)$ = 1.5 keV ,
$\langle n_e \rangle = 1.6 \times 10^{18} m^{-3}$ at 0.5MW NBI, B=2.75T]
[ICH only: τ_{pulse} = 68 s, $T_e(0) \sim T_i(0)$ = 2.0 keV,
$\langle n_e \rangle = 1.0 \times 10^{19} m^{-3}$ at 0.85MW ICH, B=2.75T].

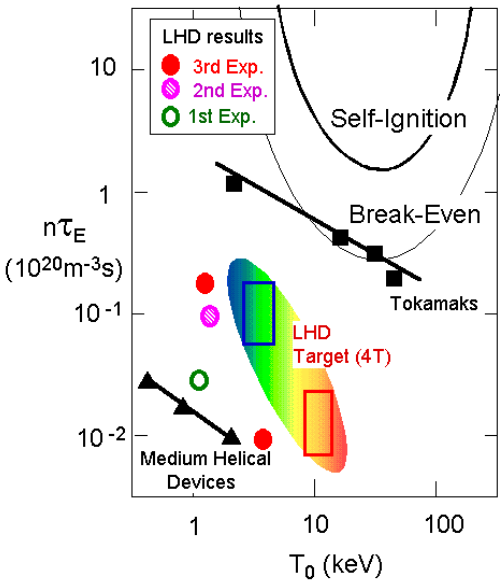

Fig.3 Plasma parameters achieved (at B<3T) and final target (at B=4T)

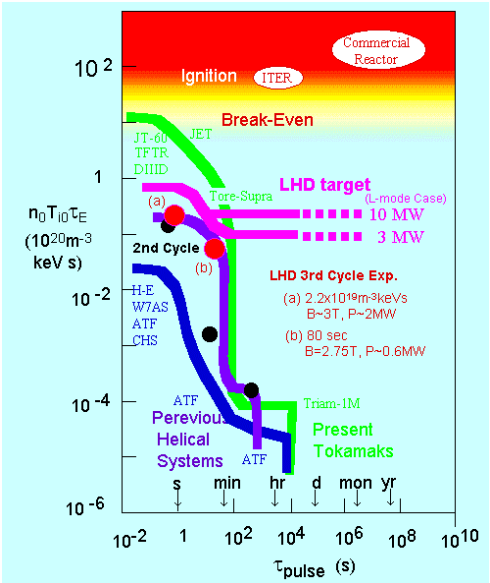

Fig. 4 Progress to Steady-State Operation

These data are plotted in the Lawson diagram (Fig.3) and the diagram of fusion triple product vs. plasma

duration (Fig.4). One of the main objectives of the LHD experiments is to demonstrate the long pulsed operation of high performance plasmas as shown in Fig.4.

4. Experimental Analysis

4.1 Confinement & Transport Physics

For experimental analysis of plasma transport, the Toroidal Transport Linkage Code (TOTAL code) [7] has been used by the self-consistent reconstruction (PRE-TOTAL code) of equilibrium using measured density and temperature profiles. The heat absorption power of NBI heating is calculated using this TOTAL code and compared with GNET code results with orbit effects [8].

(1)Global Analysis

NBI-heated hydrogen plasmas on LHD are analyzed by comparing with neoclassical ripple transport as well as anomalous transport (empirical or drift turbulence theory). The obtained global confinement time is longer than the previous scaling laws, as reported in Ref. [9].

There are four conventional global confinement scaling laws for helical systems: LHD scaling (LHD, gyro-reduced Bohm scaling (GRB), Lackner-Gotardi scaling (LG) and International Stellarator Scaling (ISS95),

$$\tau_{LHD} = 0.17 P^{-0.58} \bar{n}_e^{\,0.69} B^{0.84} R^{0.75} a^{2}, \quad (1)$$

$$\tau_{GRB} = 0.25 P^{-0.6} \bar{n}_e^{\,0.6} B^{0.8} R^{0.6} a^{2.4}, \quad (2)$$

$$\tau_{LG} = 0.17 P^{-0.6} \bar{n}_e^{\,0.6} B^{0.8} R a^{2} \iota_{2/3}^{\,0.4}, \quad (3)$$

$$\tau_{ISS95} = 0.26 P^{-0.59} \bar{n}_e^{\,0.51} B^{0.83} R^{0.65} a^{2.21} \iota_{2/3}^{\,0.4}. \quad (4)$$

Units used here are $\tau_E(s)$, $P(MW)$, $\bar{n}_e(10^{20} m^{-3})$, $B(T)$, $R(m)$, $a(m)$, respectively. These are mainly based on medium-sized helical experiments. In LHD, ~ 1.5 times higher confinement time than the ISS95 scaling is obtained which corresponds to ~ 2 times of the LHD scaling value (Fig.5).

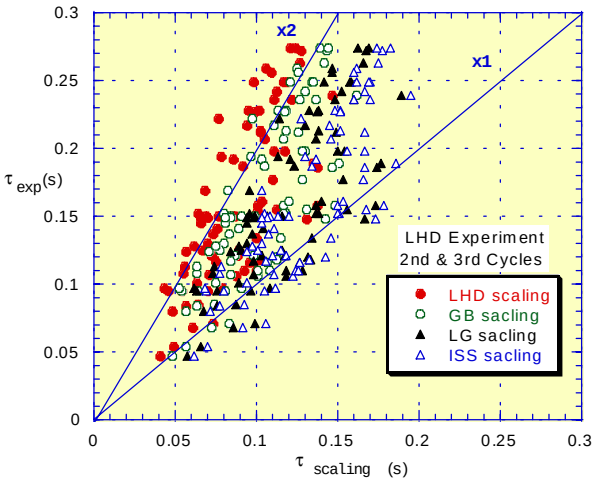

Fig. 5 LHD global confinement times vs. four helical scalings

Newly obtained global confinement scaling laws (New LHD scaling) by log-linear regression analysis are as follows:

$$\tau_{NLHD\#1} = 0.263 P^{-0.58} \bar{n}_e^{\,0.51} B^{1.01} R^{0.64} a^{2.59},$$

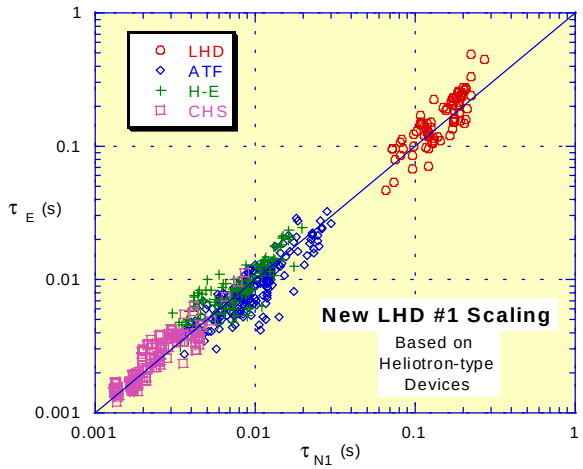

Fig. 6 Experimental confinement time of LHD vs. New LHD scaling law #1.

$$\tau_{NLHD\#2} = 0.115 P^{-0.64} \bar{n}_e^{\,0.54} B^{0.85} R^{1.02} a^{2.09}.$$

The former (Fig.6) is based on experimental data from heliotron-type devices, and the latter based on those from all helical devices including previous experimental data set of ISS-95 scalings. In this analysis we confirmed that the magnetic rotational transform does not play a statistic role, then we neglected this term.

The regression analysis is also applied to dimensionless values using normalized gyro-radius ρ_*, collisionality ν_{0*} and beta value. Here we used special analysis technique to keep Kadomtev's constraint. The obtained dimensionally-correct scalings are as follows;

$$\tau_{NLHD-D\#1} = 0.269 P^{-0.59} \bar{n}_e^{\,0.52} B^{1.06} R^{0.64} a^{2.58} \sim B^{-1} \rho_*^{\,-3.61} \nu_{0*}^{\,-0.17}$$

$$\tau_{NLHD-D\#2} = 0.115 P^{-0.64} \bar{n}_e^{\,0.54} B^{1.03} R^{1.04} a^{2.08} \sim B^{-1} \rho_*^{\,-3.41} \nu_{0*}^{\,-0.08} \beta^{-0.22}$$

Again, #1 scaling is based on only heliotron-type devices, and #2 is obtained from all database. These global scaling laws suggested the strong gyro-Bohm like features, which is different from previous conventional scaling laws (weakly gyo-Bohm like) based on only medium-sized devices.

(2) Local Analysis (radial electric field, edge pedestal and dimensionless analysis)

Local transport analysis has been carried out using 120 channel YAG Thomson electron profiles and FIR electron density profiles. Ion density and temperature profiles are assumed to be equal to those of electron, which is confirmed in some medium typical discharges. The NBI power deposition is calculated by TOTAL code, and effective thermal diffusivity χ_{eff} is defined as

$$\chi_{eff} = - (Q_{NBI}+Q_{RF}+Q_{OH} - dW/dt)/(2.5ndT/dr)$$

to avoid the uncertainty of ion temperature.

The experimental thermal diffusivity χ_{eff} was compared with neoclassical value and simple gyro-Bohm coefficient as a function of normalized plasma radius (Fig.7). The radial profile does not agree with simple gyro-Bohm coefficient. In the case of outer-shifted configuration (R>3.75m), the neoclassical value is rather high and roughly matches with the experimental χ_{eff} value as shown in the figure. On the other hand, in inward-shifted cases, the neoclassical value is around half

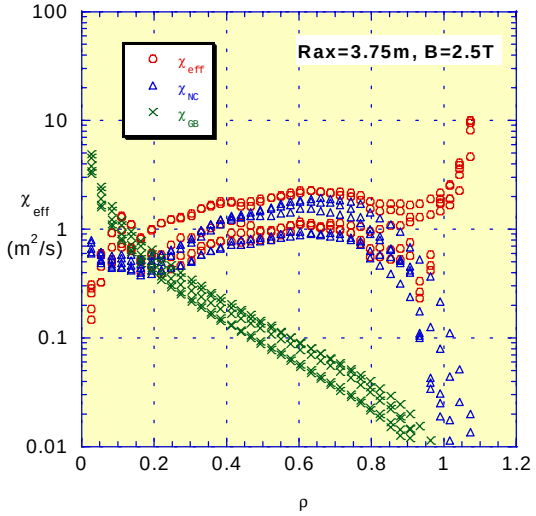

Fig.7 Thermal diffusivity of typical five shots in LHD

of the experimental value.

In the case of outer shifted configuration, the radial electric field is roughly explained by the neoclassical theory as shown in Fig.8. The lower density gives rise to the positive electric field (electron root) and the substantial reduction of ion thermal conductivity was confirmed.

The global transport was mainly determined by edge transport properties and the edge pedestal has been obtained in the LHD experiment [10] different from previous medium-sized helical devices. The core part of the confinement was found to be gyro-Bohm like as reported in Ref. [9] and the dependence of the neoclassical ripple transport is consistent with this dependence. On the other hand, the edge transport is slightly better than the gyro-Bohm dependence as shown in Fig.9. Here, we use the following dimensionally

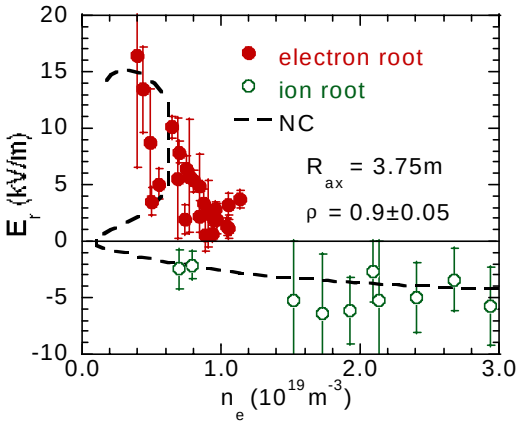

Fig. 8 Measured radial electric field compared with neoclassical ambipolar field.

normalized scaling:

$$\chi_E / (Br^2) \sim 10^c \rho_*^{c_\rho} \nu_{0*}^{c_\nu} \beta^{c_\beta} .$$

The exponents of each parameter are obtained as a function of normalized minor radius by regression analysis as shown in Fig.9. Here, plasma radius is expanded to include stochastic magnetic surfaces.

It is found that the radial distribution is weak gyro-Bohm in the core and strong gyro-Bohm near the boundary. This seems to be related to the edge pedestal of electron temperature [10]. This strong gyro-Bohm features may contribute to the enhancement of the global confinement.

These analyses suggested that the multi-mode transport feature of LHD plasma should be considered. The global confinement feature is qualitatively consistent with this strong gyro-Bohm-like local transport coefficient near the edge region.

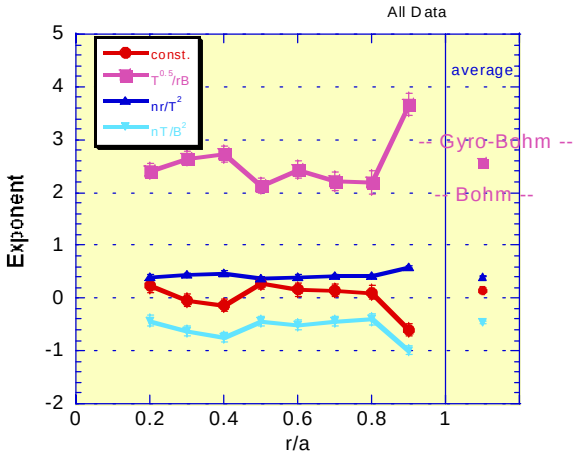

Fig.9 Exponents of dimensionless $\chi_E / (Br^2)$ scaling vs. normalized minor radius.

4.2 MHD & High Beta Physics

The inward-shifted configuration is preferable from the particle confinement and is thought to be worse from the MHD stability aspect. The Mercier criterion might be

broken in the case of Rax~3.6 m, however, the experimental evidence shows the deterioration of confinement was not observed.

To get high density and high beta plasmas, the pellet injection was used, and the highest beta value 2.4 % was achieved. The pellet injection can contribute to expand the operation regime without confinement deterioration.

In the case of high beta, the magnetic fluctuation of M=2/N=3 was observed. The detailed analysis is being performed by using CAS3D and TERPSICORE codes.

4.3 Divertor and Edge Plasma Physics

The LHD is charecterised by the three-dimentional built-in divertor[10], and the divertor tiles were changed from stainless steel to carbon tiles in the 3rd experimental campaign. This leads to the substantial reduction of impurity radiation. The limiter inserted in the plasmas surface was used to reduce plasma radius, and the global confinement depends on the minor radius scaling.

4.4 Steady-State Physics

The steady state operations by ICRF or NBI heating alone was achieved for longer than 1 minute were performed (Fig.10). In this operation, feedback control of density was manually carried out. Plasma density is $1\sim2\times10^{19}cm^{-3}$ and temperature is 1~2 keV. At present pulse length was limited by the temperature increase of protection plate for NBI injection port. The new relaxation phenomena “Breathing” was created in the long pulse operation related to the high-Z impurity accumulation. This oscillation was stopped by installing carbon divertor tiles instead of stainless steel wall.

6. Future Prospect

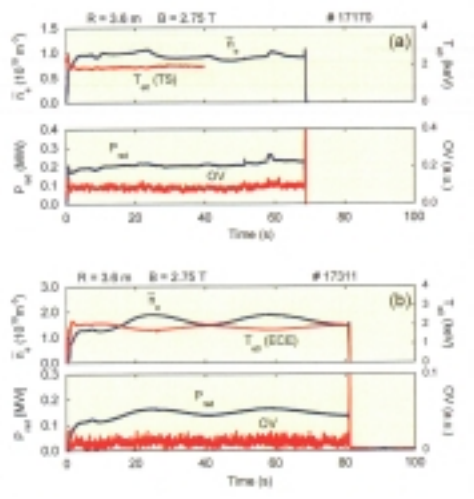

Fig. 10 Long Pulse operation in LHD

New LHD confinement scaling laws have recently been derived based on these data, and applied to the helical reactor plasma projection (Fig.11-12). For the realization of optimized fusion reactor, research and development of steady-state plasmas are crucial. We believe the LHD would demonstrate performance potential of a Heliotron configuration towards a steady-state reactor

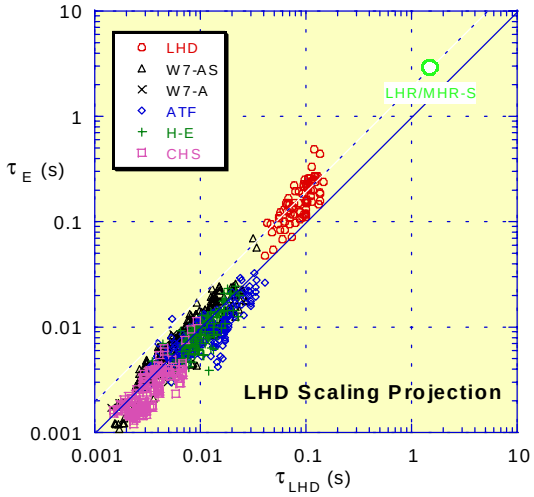

Fig.11 Reactor plasma projection based on LHD

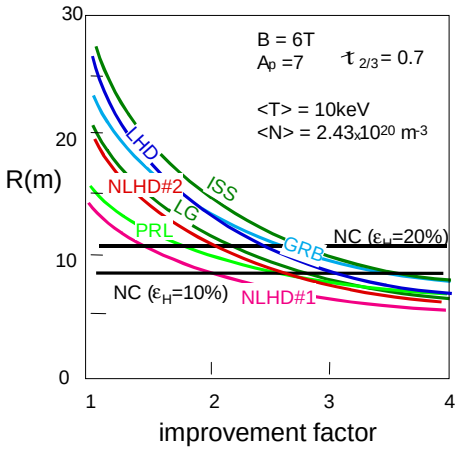

Fig. 12 Helical reactor size based on various scalings laws.

References

[1] A. Iiyoshi et al., Nucl. Fusion 39 (1999) 1245.
[2] M. Fujiwara et al. ., Nucl. Fusion 39 (1999) 1659.
[3] K. Uo, J. Phys.Soc.Jpn 16 (1961) 1380: K. Uo et al., Phys. Fluids 5 (1962) 1293.
[4] O. Motojima et al., Phys. Plasmas 6 (1999) 1843.
[5] K. Yamazaki et al., in Proc. 13th Inter. Conf. on Plasma Physics and Controlled Nuclear Fusion research (IAEA, Washington, 1-6 Octber,1990) Volume 2 p.709 (1991)
[6] M. Fujiwara et al., Nucl. Fusion 40 (2000)1157.
[7] K. Yamazaki et al., 27th EPS Conf. (2000) P4.016.
[8] S. Murakami et al., Nucl. Fusion 40 (2000) 693.
[9] H. Yamada et al., Phys. Rev. Lett. 84 (2000) 1216.
[10] N. Ohyabu et al., Phys. Rev. Lett. 84 (2000) 103.
[11]. Yamazaki et al., Fusion Engineering and Design 41 (1998) 519.